arXiv:2303.06961v2 [gr-qc] 29 Aug 2023

Observational constraints on non-minimally coupled curvature-matter models of gravity from the analysis of Pantheon data

Biswajit Jana*[1], Anirban Chatterjee †[2], Kumar Ravi ‡[1], and Abhijit Bandyopadhyay§[1]

[1]Ramakrishna Mission Vivekananda Educational and Research Institute, Belur Math, Howrah 711202, India
[2]Indian Institute of Technology Kanpur, Kanpur 208016, India

August 31, 2023

Abstract

We considered non-minimally coupled curvature-matter models of gravity in a FRW universe filled with perfect fluid and investigated its cosmological implications in the light of Pantheon compilation of 1048 Supernova Ia data points along with 54 data points from Observed Hubble Data. The non-minimal curvature-matter coupling has been introduced by adding a term $\int [\lambda R^n \mathcal{L}_m] \sqrt{-g} d^4x$ to the usual action for Einstein gravity involving the Einstein Hilbert action and minimally coupled matter action. We investigate the observational constraints on the non-minimal models by choosing two different kinds of parametrization of fluid-pressure profiles using a dimensionless parameter k. The interplay of the three parameters λ, n, k plays a pivotal role in testing the consistency of non-minimally coupled fluid-curvature scenarios with the observed data. We found there exist large domains in the (λ, n, k)-parameter space for which models with non-minimal curvature-matter mixing stand as viable cosmological models reproducing the observed features of late-time cosmic evolution. We also commented on the possibility of 'gravitationally induced particle creation' in the context of SNe Ia data.

1 Introduction

Observation of type Ia Supernovae (SNe Ia) events and their luminosity distance and redshift measurements by Riess *et.al.* [1] and Perlmutter *et.al.* [2] have independently confirmed that present universe is in an accelerated state of expansion and a transition from a decelerated to the current accelerated phase happened during it's late time phase of evolution. The reason for this late-time cosmic acceleration is attributed to a hypothetical unclustered form of energy, called 'Dark Energy' (DE), which has become a general label for the late time cosmic acceleration. On the other hand, observations of rotation curves of spiral galaxies [3], gravitational lensing [4], Bullet Cluster [5] and other colliding clusters provide evidence in favour of existence

*vijnanachaitanya2020@gmail.com
†Corresponding Author: anirbanc@iitk.ac.in & iitkanirbanc@gmail.com
‡cimplyravi@gmail.com
§abhijit.phy@gm.rkmvu.ac.in

of non-luminous matter called 'Dark Matter' (DM) in the universe. Such matter indirectly manifest their existence only through gravitational interactions. Experiments like WMAP [6] and Planck [7] have revealed that dark energy (DE) and dark matter (DM) together contribute $\sim 96\%$ of total energy density of the present-day universe, with $\sim$69% and $\sim$27% as their respective shares. The rest of the 4% contribution comes from radiation and baryonic matter.

To support his theory of the static universe, Einstein initially considered a cosmological constant term $\Lambda g_{\mu\nu}$ in the geometric part of his field equations of general relativity, but later discarded it, in favour of Hubble's observation of expanding universe. However, with the discovery of late-time cosmic acceleration in the later part of last century, the cosmological constant term again came under the spotlight because of its potential to provide a straight-way solution to Einstein's field equation resulting in an accelerated expansion. The corresponding phenomenological model that fits the observed features of cosmic acceleration is called Λ-CDM model, where CDM refers to cold dark matter content of the present universe. Unfortunately, the Λ-CDM model is plagued with the coincidence problem [8] problem and the fine-tuning problem [9]. These limitations motivate investigation of other models to account for dark energy. One class of such models are field theoretic models of dark energy involving modification of energy-momentum tensor in the Einstein's field equations due to presence of a field as one content of the universe, other than matter and radiation. Such class of models include both quintessence [10–18], and k-essence [19–26] models of scalar fields. Another class of models involve modification of the geometric part of Einstein's equations, *i.e.* the Einstein-Hilbert action in order to address issue of late time cosmic acceleration. Such models include $f(R)$ gravity models, scalar-tensor theories, Gauss-Bonnet gravity, and braneworld models of dark energy [27]. In most of these scenarios, the universe is considered to be homogeneous and isotropic at large scales, with its metric described by the Friedmann-Robertson-Walker (FRW) metric specified by a time-dependent scale factor $a(t)$ and a curvature constant K. There also exist approaches, where an inhomogeneous universe, described by a perturbed FRW metric, has been considered as the spacetime background.

In this article, we examine a model of the universe with its content as an ideal hypothetical fluid, characterised by its energy-density (ρ) and pressure (p), which is non-minimally coupled to the spacetime curvature. The non-minimal curvature-matter coupling has been introduced by adding a term $\int d^4x\sqrt{-g}\lambda R^n\mathcal{L}_m$ to the usual action for Einstein gravity involving the Einstein Hilbert action and minimally coupled matter action. R is the Ricci Scalar and $\mathcal{L}_m$ (referred to as matter Lagrangian) is the Lagrangian of the hypothetical fluid. The coupling constant (λ) and the power (n) of R in the non-minimal coupling term, are considered as the parameters of the model. We explored the constraints on these parameters from the combined analysis of Pantheon compilation of 1048 SNe Ia data points [28] and 54 data points from Observed Hubble data [29–33].

In the general framework of non-minimal models, the geometric part of Einstein's equation is altered by modifying the Einstein-Hilbert action to $\int d^4x\sqrt{-g}f(R)$, replacing R by a general function $f(R)$ [34–36]. In the context of modified $f(R)$ theories of gravity, it has been shown in [37] that the covariant derivative of energy-momentum tensor is non-vanishing ($\nabla_\mu T^{\mu\nu} \neq 0$), when a $f(R)$-$\mathcal{L}_m$ (curvature-matter) coupling is present in the theory which may cause a departure from geodesic motion manifesting existence of a new force. Consequences of such models in stellar equilibrium have been investigated in [38, 39]. An equivalence between a suitable scalar theory and the generic model with non-minimal coupling between curvature and matter have been established in [40–46]. A viability criterion to avoid instabilities in such models has been derived in [47]. The effect of curvature-matter couplings on the dynamics of particles and fields

have been analysed in [48]. In [38, 39], it has been argued that the choice $\mathcal{L}_m = p$, (p being the pressure of the matter fluid) is a 'natural' one for the matter of Lagrangian density, as it reproduces the equations of hydrodynamics of perfect fluid and in the context of curvature-matter coupling such choices result in vanishing of the extra force. However, there may be some other choices resulting in vanishing the extra force (see [36, 49] for references). In this work we have used $\mathcal{L}_m = p$ and in the framework of our considerations the field equations following from the total action involving $S_{\rm non-minimal}$ establishes connection between $a(t), \rho(t), p(t)$ through their time derivatives and various other functions like the Hubble function $H(t)$ and the Ricci scalar $R(t)$. We exploit these equations for investigating constraints on non-minimal models from the analysis of observed data.

Using a model-independent construction of Hubble's function H in terms of redshift z without invoking any specific cosmological models, we obtained the dependence of Hubble's parameter H on z from the analysis of the SNe Ia data (Pantheon + OHD). We used the FRW scale factor a to be normalised to unity at present epoch ($z = 0$). Using the relation $1/a = 1 + z$, the temporal behaviour of cosmological quantities expressed in terms of z may be equivalently expressed in terms of a or another dimensionless time parameter chosen as $\tau \equiv \ln a$, which we used in our analysis. Exploiting the profile of the Hubble's parameter for the redshift domain accessible in the SNe Ia observations, obtained from the analysis of cosmological data set, we obtain the time profile of FRW scale factor a and it's higher-order derivatives $\dot{a}$, $\ddot{a}$. This also enables us to express temporal behaviour of the Ricci scalar R and it's time derivatives which are involved in our analysis.

To investigate the observational constraints on models with non-minimal curvature-matter couplings (specified in terms of parameters λ and n in this paper), we considered two different types of fluid pressure models with temporal behaviour of pressure p modelled as $p \sim e^{ak}$ (exponential model) and $p \sim a^k$ (power law model) where k is a dimensionless parameter. Consequently the three parameters (λ, n, k) appear in the evolution equations and control the model-based computations of ρ and p. Using the observational inputs from SNe Ia data, we obtained the regions in the model parameter space (λ, n, k), for which the computed energy density (ρ) of the fluid remains positive for all time during the late time phase of evolution. This is an essential requirement for viability of cosmological models. We have also seen that there exist a small range of parameter values around $(\lambda = -0.1, n = 0.2, k = 1)$ for which the computed temporal profiles of ρ and p mimic the corresponding profiles obtained from the analysis of the data using Λ-CDM model in the context of usual minimal coupling scenario.

The non-vanishing covariant derivative of the energy-momentum tensor in the context of non-minimally coupled curvature-matter scenarios implies an exchange of energy between curvature and matter sectors. We computed the rate of the energy exchange for different benchmark values of the model parameters (λ, n, k) and found a monotonous decrease in the absolute value of the energy exchange rate as time approaches towards the present epoch. This implies that the rate of exchange of energy between the two sectors is more significant during relatively early phases of late-time cosmic evolution. The cosmological implications of curvature-matter coupling scenarios from the viewpoint of thermodynamics have been investigated in [50–52]. There it has been shown that curvature-matter coupling may be responsible for generation of a large amount of comoving entropy during late-time evolutionary phase of the universe leading to a possible interpretation of the exchange of energy between curvature and matter sector in terms of gravitationally induced particle creation in FRW universe. We have shown from the analysis of SNe Ia data that for some values of the model parameters (λ, n, k) possibility of such an interpretation is always allowed.

Rest of the paper is arranged in the following manner. In Sec. 2 we discussed the framework of non-minimally coupled $f(R)$ model in the context of a flat FRW universe and obtained the corresponding generic modified evolution equations of the universe in presence of non-minimal curvature-matter coupling. We choose two different types of fluid-pressure models, and obtained the equations corresponding to each of the models. In Sec. 3 we discussed the methodology of analysis of Pantheon + OHD data sets for obtaining temporal behaviour of different relevant cosmological quantities during the late-time phase of cosmic evolution. In Sec. 4 we presented the constraints on model parameters λ, n and k obtained by using the results extracted from the analysis of the observed data and discussed the results. We summarize the conclusions of the paper in Sec. 5.

2 Theoretical framework of curvature-matter coupling scenario

In the framework of modified theories of gravity with non-minimal curvature-matter coupling, the action may be written in the form [34]

$$S = \int \left[\frac{1}{2}f_1(R) + [1+\lambda f_2(R)]\,\mathcal{L}_m\right]\sqrt{-g}\,d^4x\,, \tag{1}$$

where $f_1(R)$ and $f_2(R)$, in general, are two arbitrary functions of the Ricci scalar R and $\mathcal{L}_m$ is the Lagrangian density for matter. g is the determinant of the spacetime metric tensor $g_{\mu\nu}$ and λ is a constant representing the strength of the non-minimal coupling between curvature term $f_2(R)$ and matter lagrangian $\mathcal{L}_m$. Following the approach of metric formalism in the context of the modified theories of gravity, the variation of the action with respect to the field $g_{\mu\nu}$ yields the modified field equations as

$$\begin{aligned} F_1 R_{\mu\nu} - \frac{1}{2}f_1 g_{\mu\nu} - \nabla_\mu\nabla_\nu F_1 + g_{\mu\nu}\Box F_1 &= (1+\lambda f_2)T_{\mu\nu} - 2\lambda F_2\mathcal{L}_m R_{\mu\nu} \\ &\quad +2\lambda(\nabla_\mu\nabla_\nu - g_{\mu\nu}\Box)\mathcal{L}_m F_2\,, \end{aligned} \tag{2}$$

where we put $8\pi G = 1$ (G = Gravitational Constant), $F_i = df_i/dR$ $(i = 1, 2)$ and $T_{\mu\nu}$ is the matter energy-momentum tensor given by

$$T_{\mu\nu} = -\frac{2}{\sqrt{-g}}\frac{\delta(\sqrt{-g}\mathcal{L}_m)}{\delta(g^{\mu\nu})}\,. \tag{3}$$

In this article, we investigated the scenario of non-minimal coupling between curvature and matter with geometric part of field equation driven by pure Einstein gravity *i.e.* with $f_1(R) = R$ and considered the matter part to be non-minimally coupled (with coupling strength λ) to curvature through the function $f_2(R) = R^n$ (where n is some constant). In this model, the matter part of the universe is described by a perfect fluid characterised by energy density ρ and pressure p. Following the comprehensive discussion in [35, 36], we assume $\mathcal{L}_m = p$, which is a 'natural choice' for Lagrangian density for perfect fluids, which correctly reproduces the hydrodynamical equations for a perfect fluid. This particular choice has interesting consequences in the analysis of curvature-matter coupling scenarios implying vanishing of extra force owing to departure from motion along the geodesic which may arise due to non-vanishing covariant derivative of $T_{\mu\nu}$ in the context of curvature-matter coupling [37]. There are, however, other choices of $\mathcal{L}_m$ investigated in [34, 36].

We conducted an exploration of the intricacies associated with non-minimal coupling between the curvature and matter by employing a power law form of the function $f_2(R) = R^n$, where n is

a constant exponent. Apart from the strength of the coupling λ, such consideration introduces a single additional parameter n into the analytical framework. These two parameters (λ, n), along with a third parameter k, used to express temporal variation of the fluid pressure, constitute a 3-dimensional parameter space (λ, n, k) facilitating the exploration of non-minimally coupled theories with fluids having a wide range of pressure variation modes, with an optimum number of parameters. It's important to recognize that the power law representation $f_2(R) = R^n$ for any real n may be represented through the expansion of $f_2(R)$ around a non-zero reference point $R = R_0$ in the form of infinite series: $f_2(R) = \sum_m c_m(R - R_0)^m$, where m is an integer, encompassing negative values as well, when n is negative. Nevertheless, the scenario of non-minimal couplings may theoretically be explored using particular $f_2(R)$ expressions consisting of a finite number of terms incorporating diverse integral powers (both positive and negative) of R. Consideration of such forms would then introduce more parameters (the coefficients of the different integral powers of R) into the analysis scheme compared to the power-law version of $f_2(R)$. Under such considerations, obtaining observational constraints on non-minimally coupled scenarios necessitate exploring parameter spaces of significantly higher dimensions. This also requires assessment of distinct parameter combinations for each specific expression of $f_2(R)$ to encompass the wide spectrum of $f_2(R)$ patterns. In contrast, opting for the power law form $f_2(R) = R^n$ (as adopted for this study), covers an alternative array of varied $f(R)$ profiles (demonstrating either monotonic increase or decrease) achieved solely by modifying the exponent n. This choice renders the investigation more manageable in terms of the triad (λ, n, k). We have also come to recognize that the adoption of the power law form $f_2(R) = R^n$ has proven advantageous in terms of computational time and efficiency, in pinpointing the precise value of n for which the evaluated temporal profile of energy density and fluid pressure mimic the corresponding patterns seen in the Λ-CDM model. To summarise our considerations for the present analysis, we have chosen $f_1(R) = R, f_2(R) = R^n, F_2(R) = nR^{n-1}, \mathcal{L}_m = p$. For such choices Eq. (2) can be expressed as

$$R_{\mu\nu} - \frac{1}{2}Rg_{\mu\nu} = (1 + \lambda R^n)T_{\mu\nu} - 2\lambda(nR^{n-1})pR_{\mu\nu} + 2\lambda(\nabla_\mu\nabla_\nu - g_{\mu\nu}\Box)p(nR^{n-1})\,. \quad (4)$$

The energy density ρ and pressure p of the fluid are respectively obtained from '00' and 'ii' components of the energy-momentum tensor $T_{\mu\nu}$. The '00' component of Eq. (4) is

$$R_{00} - \frac{1}{2}Rg_{00} = (1 + \lambda R^n)T_{00} - 2\lambda p(nR^{n-1})R_{00} - 6\lambda H(\dot{p}nR^{n-1} + pn(n-1)R^{n-2}\dot{R})\,. \quad (5)$$

For a FRW spacetime background the above equation takes a form which after some rearrangements may be written as

$$\rho = \frac{1}{1 + \lambda R^n}\left[3H^2 + 6n\lambda\{(n-1)HR^{n-2}\dot{R} - (H^2 + \dot{H})R^{n-1}\}p + 6n\lambda HR^{n-1}\dot{p}\right]. \quad (6)$$

On the other hand, the 'ii'-component of Eq. (4) is

$$R_{11} - \frac{1}{2}Rg_{11} = (1 + \lambda R^n)T_{11} - 2\lambda pnR^{n-1}R_{11} + 2\lambda(\nabla_1\nabla_1 - g_{11}\Box)(pnR^{n-1})\,, \quad (7)$$

which in the FRW spacetime background takes the form

$$\begin{aligned} -(2\dot{H} + 3H^2) = {} & \Big[(1 + \lambda R^n - 2\lambda nR^{n-1}(\dot{H} + 3H^2) + 4n(n-1)\lambda HR^{n-2}\dot{R} \\ & + 2\lambda\{n(n-1)(n-2)R^{n-3}\dot{R}^2 + n(n-1)R^{n-2}\ddot{R}\}\Big]p \\ & + 4n\lambda\Big\{HR^{n-1} + (n-1)R^{n-2}\dot{R}\Big\}\dot{p} + 2n\lambda R^{n-1}\ddot{p}\,. \end{aligned} \quad (8)$$

In the framework of curvature-matter coupling in FRW spacetime background Eqs. (6) and (8) are the master equations. Note that Eqs. (6) and (8) involve time derivatives of the pressure

of the fluid which is a consequence of the non-minimal curvature-matter coupling. Setting the non-minimal coupling constant $\lambda = 0$ in the master equation, we retrieve the usual Friedmann equations which do not contain any derivative term of pressure.

To investigate the observational constraints on such curvature-matter coupling models, we considered two types of fluid pressure models with specific temporal profile of the fluid pressure. In FRW background, we choose to express the modelled temporal profiles of the fluid pressure in terms of the FRW scale factor. We discuss below the two models referred to as exponential and power-law models as per the nature of dependences of the pressure on the scale factor in the corresponding models.

Exponential model : In this model we take the fluid pressure p as $p = p_0 \exp(ak)$, where k is a dimensionless parameter and p_0 is a constant having the dimension of pressure. $p_0 e^k$ gives the pressure of the fluid at present epoch $a = 1$, in this model. We then have $\dot{p} = kp\dot{a}$ and $\ddot{p} = k^2 p\dot{a}^2 + kp\ddot{a}$. Using $\dot{p} = kp\dot{a}$ in Eq. (6), we may express the energy density for a given value of λ, n, k and pressure p corresponding to this model as

$$\rho(t;\lambda,n,k) = \frac{1}{1+\lambda R^n}\left[3H^2 + 6n\lambda\Big\{(n-1)HR^{n-2}\dot{R} - (H^2+\dot{H})R^{n-1} + kHR^{n-1}\dot{a}\Big\}p\right] . \quad (9)$$

Note that the above equation also implies dependence of the $\rho(t;\lambda,n,k)$ on the parameter p_0 due to occurrence of the pressure term $p = p_0 \exp(ak)$ in the right hand side of Eq. (9). But note that, we may use Eq. (8) with $\dot{p} = kp\dot{a}$ and $\ddot{p} = k^2 p\dot{a}^2 + kp\ddot{a}$ to express the pressure $p = p_0 \exp(ak)$ as

$$\begin{aligned} p(t;\lambda,n,k) &= -(2\dot{H}+3H^2)\Big[(1+\lambda R^n - 2\lambda n R^{n-1}(\dot{H}+3H^2) + 4n(n-1)\lambda H R^{n-2}\dot{R} \\ &\quad +2\lambda\Big\{n(n-1)(n-2)R^{n-3}\dot{R}^2 + n(n-1)R^{n-2}\ddot{R}\Big\} \\ &\quad +4n\lambda k\Big\{HR^{n-1} + (n-1)R^{n-2}\dot{R}\Big\}\dot{a} + 2n\lambda k R^{n-1}(k\dot{a}^2 + \ddot{a})\Big]^{-1} . \end{aligned} \quad (10)$$

We may now use this expression of Eq.(10) for p in Eq. (9) to get rid of its explicit p_0 dependence. So that $\rho(t;\lambda,n,k)$ in Eq. (9) is computable at any t for any given choice of parameter set (λ, n, k).

Power-law model : In this model we take $p = p_0 a^k$, where k is again a dimensionless constant and p_0 is a constant, which in this model gives the value of pressure at present epoch ($a = 1$). Here we thus have $\dot{p} = kpH$ and $\ddot{p} = p(k^2H^2 + k\dot{H})$. Using $\dot{p} = kpH$ in Eq. (6) we may similarly express the energy density for a given set of values of λ, n, k and pressure p as

$$\rho(t;\lambda,n,k) = \frac{1}{1+\lambda R^n}\left[3H^2 + 6n\lambda\Big\{(n-1)HR^{n-2}\dot{R} - (H^2+\dot{H})R^{n-1} + kH^2R^{n-1}\Big\}p\right] . \quad (11)$$

Here also, to get rid of the parameter p_0 which appears in the pressure term $p = p_0 a^k$ in the right hand side, we exploit the Eq. (8) with $\dot{p} = kp\dot{a}$ and $\ddot{p} = k^2 p\dot{a}^2 + kp\ddot{a}$ to express the instantaneous values of pressure $p = p_0 a^k$ in terms of parameters (λ, n, k) as

$$\begin{aligned} p(t;\lambda,n,k) &= -(2\dot{H}+3H^2)\Big[(1+\lambda R^n - 2\lambda n R^{n-1}(\dot{H}+3H^2) + 4n(n-1)\lambda H R^{n-2}\dot{R} \\ &\quad +2\lambda\Big\{n(n-1)(n-2)R^{n-3}\dot{R}^2 + n(n-1)R^{n-2}\ddot{R}\Big\} \\ &\quad +4n\lambda\Big\{HR^{n-1} + (n-1)R^{n-2}\dot{R}\Big\}kH + 2n\lambda R^{n-1}(k^2H^2 + k\dot{H})\Big]^{-1} \end{aligned} \quad (12)$$

and use this expression for pressure p in Eq. (11) to evaluate instantaneous value of energy density for any given set of parameters (λ, n, k).

Apart from the model parameters (λ, n, k), the expressions for ρ and p (in both exponential and power law models) involve other cosmological parameters - the FRW scale factor a, its time derivatives, the Hubble parameter H and its time derivatives, the Ricci scalar $R(= 12H^2 + 6\dot{H})$ and its time derivatives. We have obtained the temporal behaviour of all these cosmological quantities during the late time phase of the cosmic evolution from a combined analysis of recently released Pantheon (SNe Ia) data. The accessible range of red-shift in the date sets corresponding to Pantheon data set is $0 \leq z \leq 2.3$ corresponds to a cosmic time domain $0.23 \leq t \leq 1$, where t is normalised to unity at the present epoch. Using the time dependences of the said cosmological quantities as extracted from the observed data, we obtained the temporal behaviour of the energy density and pressure of the fluid for both exponential and power law models using Eqs. (9), (10), (11) and (12). We obtained range of values of parameters (λ, n, k) for which the evaluated values of energy density function $\rho(t; \lambda, n, k)$ remains positive at all time. The reach of the recent SNe Ia data accommodates within itself the scenario of matter-curvature non-minimal coupling for the constrained values of the model parameters.

3 Obtaining constraints on the cosmological quantities from combined analysis of Pantheon and Observed Hubble data

The cosmological data from Supernovae Ia observation provides information about late time cosmic evolution of the universe. In this section we briefly outline the technical details of the analysis of the observational data which involves Pantheon (SNe Ia) data involving 1048 data points and Observed Hubble Data (OHD) involving 54 data points [29–33] and discussed how we finally extracted the temporal behaviour of the FRW scale factor a and its derivatives which are essential ingredients for constraining the non-minimally coupled matter-curvature models as discussed in Sec. 2.

The SNe Ia data provides an estimation of luminosity distances (d_L) at the redshift values (z) corresponding to different SNe Ia events. The 'Pantheon Sample' [28] is a compilation of the subset of 279 PS1 SNe Ia data points (over a redshift range $0.03 < z < 0.68$) along with useful compilations of SNe Ia data from SDSS [53], SNLS [54], various low-z [55], and HST samples [56] to form the largest combined sample of SNe Ia consisting of a total of 1048 SNe Ia over the redshift range $0.01 < z < 2.3$. We have used the above mentioned data samples to construct the Hubble function $H(z)$ without invoking any specific cosmological models. For such a model-independent construction, we use Padé approximant of order (2,1) [57] for luminosity distance function, which is a closed-form parametrization of the luminosity distance in terms of the redshift expressed as

$$d_L(z, \alpha, \beta) = \frac{c}{H_0}\left(\frac{z(1+\alpha z)}{1+\beta z}\right), \tag{13}$$

where c is the speed of light and H_0 is the value of the Hubble parameter at the present epoch which may be defined through a dimensionless quantity h by $H_0 = 100h$ km s^{-1} Mpc^{-1}. α and β are the parameters to be determined from cosmological data. The Pantheon sample of 1048 data points provide the redshift, apparent magnitude (m) at maximum brightness of the SNe Ia events, and also the covariance and correlations among the different data points. The observed data at any redshift z_i is expressed through the distance modulus $\mu_{\rm obs}(z_i)$ which is given in terms of the absolute magnitude M and observed apparent magnitudes $m_{\rm obs}(z_i)$ by the relation

$$\mu_{\rm obs}(z_i) \;=\; m_{\rm obs}(z_i) - M\,. \tag{14}$$

The form of the distance modulus $\mu_{\rm th}(z,\alpha,\beta)$ corresponding to the assumed parametric form of $d_L(z,\alpha,\beta)$ given in Eq. (13) may be obtained by using the expression

$$\mu_{\rm th}(z,\alpha,\beta) \;=\; 5\log_{10}\left[\frac{H_0 d_L(z,\alpha,\beta)}{c}\right]+\mu_0 = 5\log_{10}\left[\frac{z(1+\alpha z)}{1+\beta z}\right]+\mu_0\,, \tag{15}$$

where $\mu_0 = 42.38 - 5\log_{10} h$. Computing $\mu_{\rm th}(z_i,\alpha,\beta)-\mu_{\rm obs}(z_i)$ for the data points i, we may find the χ^2-function for the SN-data date defined by the relation

$$\chi^2_0 \;=\; \sum_{i,j=1}^{N}\Big[\mu_{\rm th}(z_i,\alpha,\beta)-\mu_{\rm obs}(z_i)\Big]C^{-1}_{ij}\Big[\mu_{\rm th}(z_j,\alpha,\beta)-\mu_{\rm obs}(z_j)\Big]\,, \tag{16}$$

where $N = 1048$ is the total number of data points considered and C is the covariance matrix of the data as released in [28], which includes both statistical and systematic uncertainties. Using Eqs. (14) and (15), the quantities $\mu_{\rm th}-\mu_{\rm obs}$ appearing in Eq. (16) may be expressed as

$$\Big[\mu_{\rm th}(z_i,\alpha,\beta)-\mu_{\rm obs}(z_i)\Big] \;=\; 5\log_{10}\left[\frac{z_i(1+\alpha z_i)}{1+\beta z_i}\right]-m_{\rm obs}(z_i)+M'\,, \tag{17}$$

where $M' \equiv \mu_0 + M = 42.38 - 5\log_{10} h + M$. Since the Pantheon data set comprises of apparent magnitudes only so this data-set alone cannot constrain H_0. The parameter $H_0 (= 100h$ km s^{-1} Mpc$^{-1})$ enters in the χ^2 function through the parameter M'. Marginalising over the parameter M', called the nuisance parameter, we define an appropriate χ^2 function for this data set [58] as

$$\chi^2_{\rm SN} \;=\; -2\ln\int_{-\infty}^{\infty}\exp\left[-\frac{1}{2}\chi^2_0(\alpha,\beta,M')\right]dM'\,, \tag{18}$$

which may be put in the following form

$$\chi^2_{\rm SN} \;=\; P-\frac{Q^2}{R}+\ln(R/2\pi)\,, \tag{19}$$

where $P = (m_{\rm obs}-m_{\rm th})^T C^{-1}(m_{\rm obs}-m_{\rm th})$, $Q = (m_{\rm obs}-m_{\rm th})^T C^{-1}\mathbf{1}$ and $R = \mathbf{1}^T C^{-1}\mathbf{1}$. Here $(m_{\rm obs}-m_{\rm th})$ represents a column matrix of the residuals with $i^{\rm th}$ entry as $\Big[m_{\rm th}(z_i,\alpha,\beta)-m_{\rm obs}(z_i)\Big]$ and $(m_{\rm obs}-m_{\rm th})^T$ denotes the corresponding transposed matrix. $m_{\rm obs}(z_i)$ is the observed value of apparent magnitude at redshift z_i and corresponding theoretical value $m_{\rm th}(z)$ is given by the formula $m_{\rm th}(z) = 5\log_{10}\left[\frac{z(1+\alpha z)}{1+\beta z}\right]+25$. The symbol $\mathbf{1}$ represents a column array of ones of same length as $m_{\rm obs}$.

In our analysis we have also used 31 redshift *vs* Hubble parameter data points from chronometer observations [59] and 23 data points from the line of sight Baryonic Acoustic Oscillations(BAO) data [29–33]. For a cosmological model-independent construction of the Hubble parameter, we use the expression

$$H(z,\alpha,\beta) = \left[\frac{1}{c}\frac{d}{dz}\left\{\frac{d_L(z,\alpha,\beta)}{(1+z)}\right\}\right]^{-1}\,, \tag{20}$$

where $d_L(z,\alpha,\beta)$ is as given in Eq. (13). The residual for the Observed Hubble data involving total 54 data points fitting is given by

$$\chi^2_{\rm OHD} \;=\; \sum_{i=1}^{54}\left[\frac{H(z_i,\alpha,\beta)-H_{\rm obs}(z_i)}{\sigma_i}\right]^2\,, \tag{21}$$

where $H_{\rm obs}(z_i)$ and σ_i give the observed value of Hubble parameter and its corresponding uncertainty respectively at redshift z_i corresponding to the $i^{\rm th}$ data point of OHD data set.

To get estimates of the parameters H_0, α, β along with their uncertainties, we perform a Markov chain Monte Carlo (MCMC) Bayesian parameter estimation using a uniform prior to all the parameters. We used the python packages, available in the public domain, *emcee* [60] and *GetDist* [61] for generating generate MCMC samples and for plotting posterior distributions of H_0, α, and β respectively. After performing various tests for the independence, convergence of the MCMC samples and thinning of the samples accordingly, we get following estimates from the combined analysis of Pantheon data and OHD. In Fig. 1 we presented the posterior distribution plot of H_0, α, and β which depicts the corresponding 1σ and 2σ uncertainties for these parameters.

$$\alpha = 1.23^{+0.06}_{-0.05}, \quad \beta = 0.45^{+0.03}_{-0.03}, \quad \text{and} \quad H_0 = 68.31^{+1.03}_{-1.03}\ \text{km s}^{-1}\ \text{Mpc}^{-1}\,. \tag{22}$$

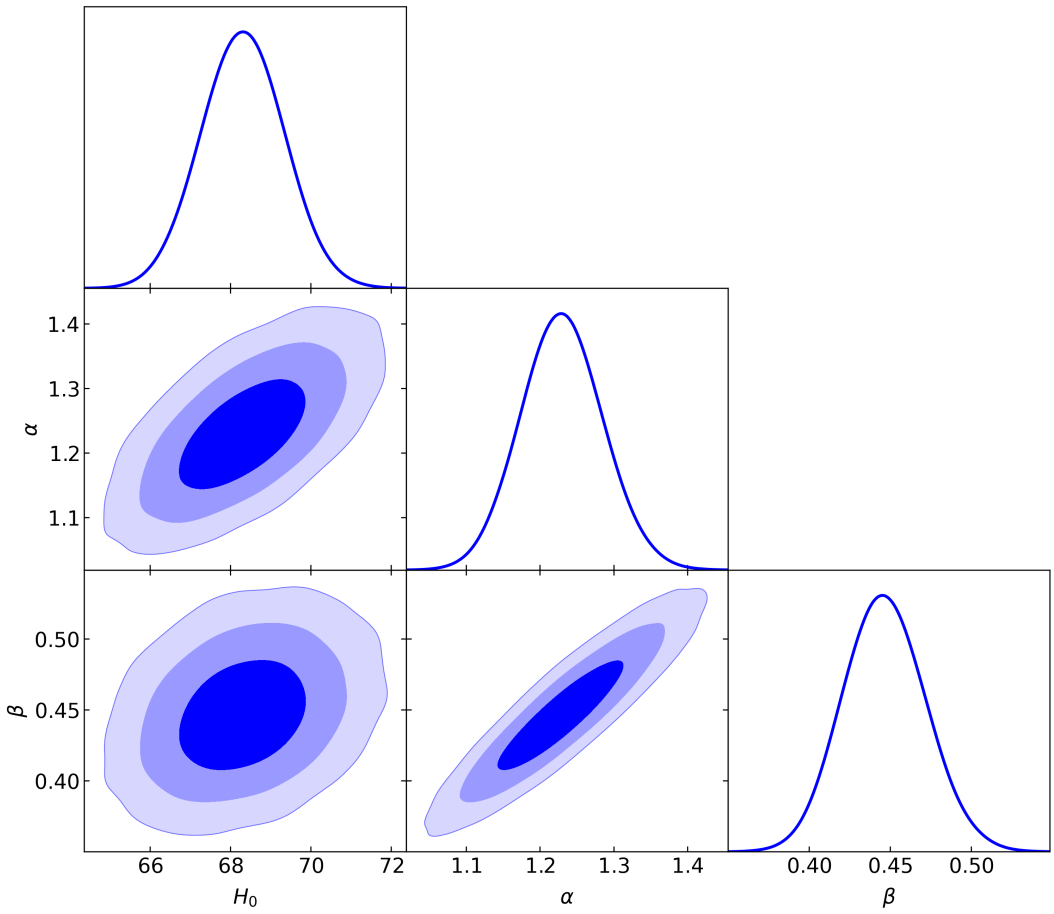


Figure 1: The posterior distribution plot of H_0, α, and β

The obtained best-fit values of the parameters α, β and H_0 along with their respective uncertainties are then exploited to compute the redshift dependences (temporal profiles) of the Hubble parameter H and the normalised Ricci Scalar R/H_0^2 making use of Eq. (20) and $R = 12H^2 + 6\dot{H}^2$. We have shown the plots of H and R/H_0^2 vs z respectively in the left and right panels of Fig. 2. The solid lines in Fig. 2 correspond to the best-fit curve of each figure. The 1σ and 3σ uncertainties in the obtained dependences are also shown by dashed lines.

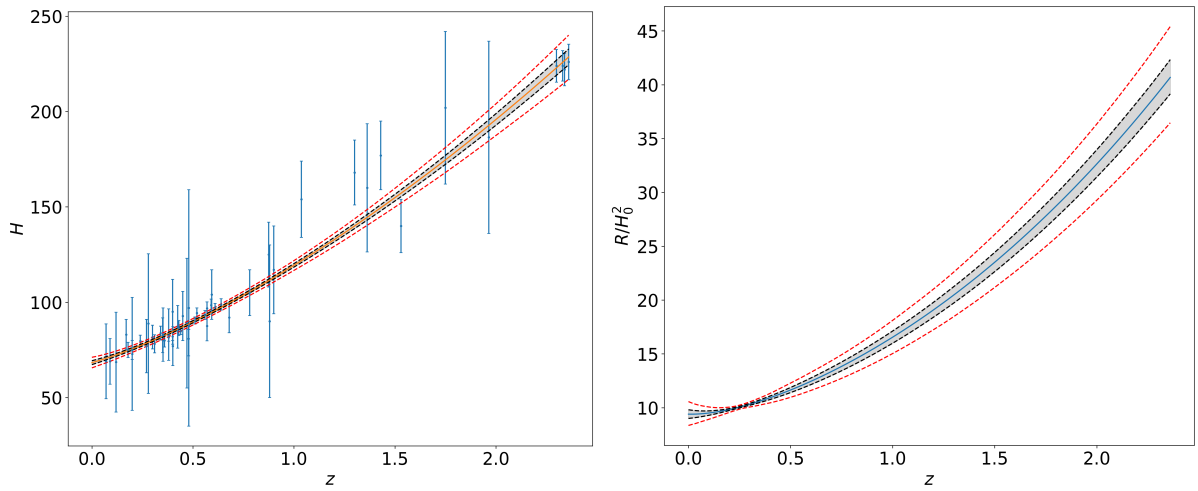


Figure 2: Left Panel: Best-fit curve with 1σ and 3σ uncertainties obtained for $H(z)$ vs z from analysis of Pantheon + OHD data. Observed values of H (with error bars) corresponding to the 54 data points from OHD are also shown. Right Panel: Best-fit curve with 1σ and 3σ uncertainties obtained for $R(z)/H_0^2$ vs z from the analysis

The profile of the $H(z)$ function, thus extracted from the analysis of the observational data, may further be used to compute the temporal behaviour of the FRW scale factor $a(t)$ and it's time derivatives $\dot{a}$, $\ddot{a}$. The steps for this computation are briefly outlined below. The FRW scale a is normalised to unity at the present epoch ($z = 0$) and is related to redshift by the relation $1/a = 1 + z$. Since $H = \dot{a}/a$, this corresponds to $dt = -\frac{dz}{(1+z)H(z)}$ which on integration gives

$$\frac{t(z)}{t_0} \;=\; 1 - \frac{1}{t_0}\int_z^0 \frac{dz'}{(1+z')H(z')}\,, \tag{23}$$

where t_0 denotes the present epoch which is also normalised to unity at present epoch ($t_0 = 1$). Using the values of $H(z)$ corresponding to the $H(z)$ profile as depicted in left panel of Fig. 2, we numerically compute the integral in the right hand side of Eq. (23). Using Eq. (23) and the equation $1/a = 1 + z$, we may obtain numerically compute simultaneous values of a and t at any given redshift z which amounts to obtaining values of $a(t)$-vs-t eliminating z from the two equations. This leads to extraction of the temporal behaviour of the scale factor $a(t)$ from the observational data for the late time domain of the cosmic evolution accessible through Supernova Ia observations.

To perform this, we vary z from zero (present epoch) to ~ 2.4 (*i.e.* within the domain of z relevant for Pantheon data set) in small steps ($\Delta z = 0.01$). We numerically compute value of the integral in Eq. (23) and also the value of $a(z) = 1/(1 + z)$ at each z-step, to obtain the sets of values $(t(z), a(z))$ at each step. Using the normalisation of scale factor $a(t)$ as $a = 1$ at present epoch ($z = 0$ or $t = 1$), we found that the range $0 < z < 2.3$ corresponds to t-range: $1 > t(z) > 0.23$. Values of $(t(z), a(z))$ over the domain $0 < z < 2.3$ provides temporal behaviour of scale factor over the time range $0.23 < t < 1$. Using the obtained profile of $a(t)$, we also obtain a profile of $\dot{a}(t)$ and $\ddot{a}(t)$ using direct numerical differentiation techniques. We have shown the plots of the profiles $a(t)$, $\dot{a}(t)$ and $\ddot{a}(t)$ respectively in the left, middle and right panels of Fig. 3. The appearance of a minima at $t \sim 0.53$ in the time-profile of $\dot{a}$ (middle panel) or equivalently,the corresponding change of sign of $\ddot{a}$ in the plots of right panel figure clearly signifies the transition from decelerated to an accelerated phase of expansion during the late time of cosmic evolution.

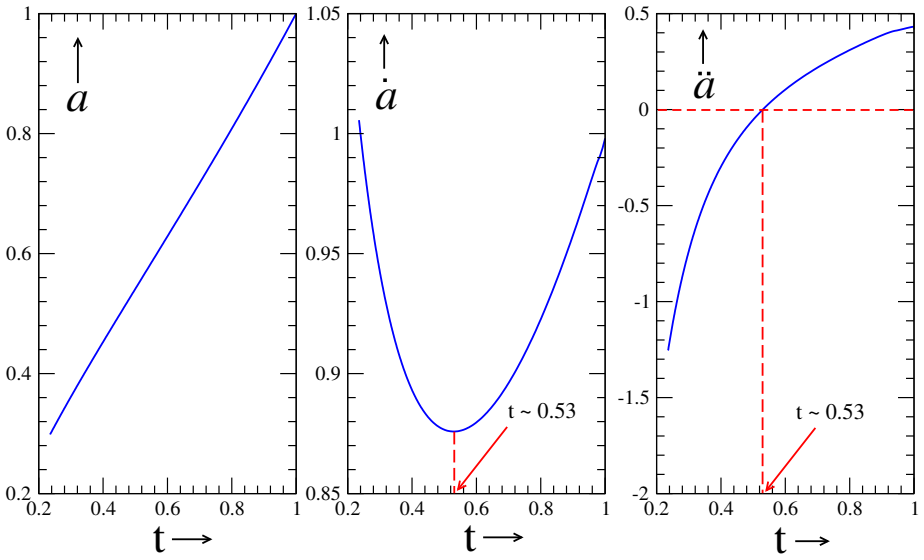


Figure 3: Temporal behaviour of scale factor at the best-fit of Pantheon data sets

4 Results and Discussion

In this section we present the results regarding the observational constraints on non-minimally coupled curvature-matter models for two types of fluid pressure scenarios - the exponential and power law profiles as discussed in Sec. 2. The energy density of the fluid in the context of the two scenarios are given by Eqs. (9) and Eq. (11) respectively. The temporal evolution of the energy density $\rho(t;\lambda,n,k)$ has been expressed in terms of cosmological quantities like $a, \dot{a}, H, R$ *etc.* The expression also involves the dimensionless parameters: λ, n, k. Temporal profile of the cosmological quantities during the late time phase of the cosmic evolution have been extracted from observational data and presented in Sec. 3. The constant λ gives the strength of the non-minimal coupling between matter and curvature sector. The parameter k is involved in the modelling of fluid pressure and n denotes the power of the gravity term ($f_2(R) = R^n$) that is coupled to the matter lagrangian. The energy density of a fluid always being a positive quantity, the constraints on parameters (λ, n, k) for such models come from imposition of the constraint $\rho(t;\lambda,n,k) > 0$ for all t, where ρ at any t is evaluated with the values of cosmological quantities $(a, \dot{a}, H, R)$ at that t as obtained from the analysis of observational data.

We presented the observational constraints on the parameters (λ, n, k) by depicting the allowed area of the k-n parameter space for certain chosen values of the coupling parameter λ. Obtaining these allowed regions required a thorough scanning of the parameter space and the pragmatic approach involves predefining a range for the parameters n and k that requires scanning, alongside selecting a scope for the parameter λ. In this study, we purposefully choose the relevant range of the coupling strength $|\lambda|$ spanning from 0.1 to 10. This choice is motivated by our intention to comprehensively investigate the cumulative impact of all terms involved in the primary action. When the coupling strength takes on higher values ($|\lambda| > 10$), the significance of $f_1(R) = R$ diminishes compared to the prevalence of other terms. Conversely, for lower coupling values ($|\lambda| < 0.1$), the impact of non-minimal coupling becomes overshadowed by the prominence of other terms within the action. We, thus, purposefully choose to focus on benchmark values of λ that fall within the above mentioned range in order to illustrate our findings. When determining the range of parameter space to be scanned for obtaining observationally allowed ranges of n and k, we systematically investigated various distinct regions within the parameter

space. In the parameter space domain corresponding to exceedingly high or low values of n and k (beyond the limits of $-10 \leqslant n \leqslant 10$ and $-20 \leqslant k \leqslant 20$), we did not observe any distinctive, disconnected and closed domains which are observationally allowed or disallowed, that could provide novel and significant insights into those specific portions of the parameter space. Hence, in presenting the outcomes in Fig. 4, we have depicted a confined region within the parameter space, defined by $-10 \leqslant n \leqslant 10$ and $-20 \leqslant k \leqslant 20$. Within this defined realm, conspicuous patterns of various disallowed domains have come to light, providing a scope to comprehend the interrelations between the parameters n and k in congruence with observations.

We presented the results for both the fluid pressure models (exponential and power law) for four benchmark values: $\lambda = -0.1, 0.1, 1, 10$. The allowed regions in the parameter space, which correspond to $\rho > 0$, are shown by shaded regions in Fig. 4. The left and right panels of the figure correspond to the parameter space constraints obtained for exponential and power-law fluid-pressure models respectively. We observe from Fig. 4 that, for both classes of fluid pressure models, a wide region of the explored portion of the parameter space is allowed which in turn implies that the Supernova Ia data (Pantheon) and Observed Hubble data robustly allows non-minimally coupled matter-curvature scenarios. However for negative values of λ, the positive values of the n (which is the power of R in the matter-curvature coupling term) gets severely constrained.

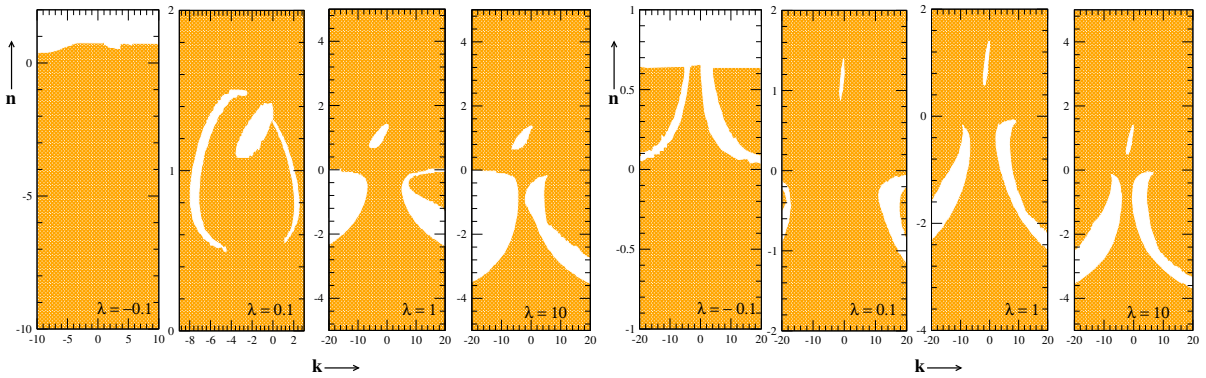


Figure 4: Left Panel: Allowed region of k-n parameter space for $\lambda = -0.1, 0.1, 1, 10$ for *exponential* model (discussed in text). Right Panel: Allowed region of k-n parameter space for $\lambda = -0.1, 0.1, 1, 10$ for *power law* model (discussed in text)

In Eqs. (10) and (12) we have also expressed the temporal profile of the fluid pressure $p(t; \lambda, n, k)$ for exponential and power law models respectively. To see the time evolution of energy density and pressure in the context of non-minimally coupled matter-curvature scenarios we have shown the plots of the temporal profile of energy density and pressure for both fluid models in Fig. 5 for certain benchmark values of the parameter set (λ, n, k) chosen from the allowed domains corresponding to both fluid models.

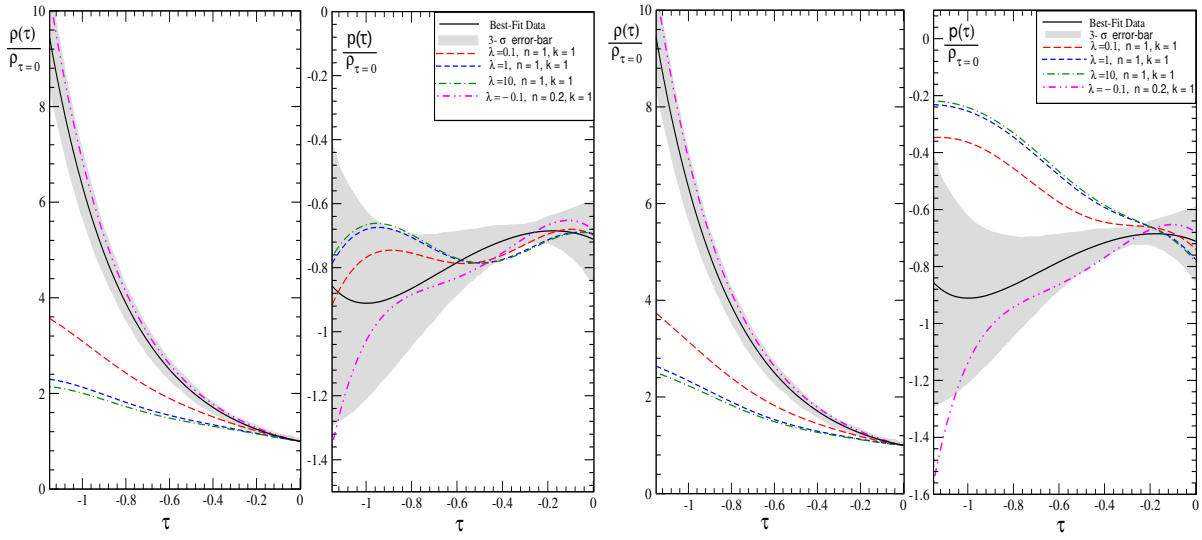


Figure 5: Left Panel: Temporal behaviour of energy density (in the left) and pressure (in the right) for different benchmark values of the parameters (λ, n, k) for *exponential* model (discussed in text). Right Panel: Temporal behaviour of energy density (in the left) and pressure (in the right) for different benchmark values of the parameters (λ, n, k) for *power law* model (discussed in text)

For convenience, we use a dimensionless time parameter τ defined as $\tau = \ln a$ to show the time profile of the energy density and pressure in Fig. 5. The late-time domain of cosmic evolution is accessible in SNe Ia observations of Pantheon sample which corresponds to the range $-1.18 \leq \tau \leq 0$ with $\tau = 0$ corresponding to the present epoch ($a = 1$). We also normalise the energy density $\rho(\tau)$ and pressure $p(\tau)$ by the energy density value at present epoch ρ_0 to get rid of dimensions and plotted $\rho(\tau)/\rho_0$ and $p(\tau)/\rho_0$ as a function of τ for different choices of the parameters k, n, λ. In the left (right) panel of Fig. 5 we showed these plots for $\rho(\tau)/\rho_0$ and $p(\tau)/\rho_0$ and for the exponential (power law) model. All the curves are shown in Fig. 5 correspond to $k = 1$. The 4-curves in each of plots correspond to 4 different choices of the set (λ, n) *viz.* (0.1, 1), (1,1), (10,1), (-0.1,0.2), all of which are well within the observationally allowed region of parameter values for each of the models as depicted in Fig. 4. For comparison, in these plots, we also showed the best-fit (solid curve) and 3σ uncertainties (shaded region) of the energy density and pressure profiles that result from usual analysis of observational data corresponding to the $\Lambda-$CDM model.

We see from Fig. 5 that, for exponential and power-models the energy density and pressure profile corresponding to parameter values $(\lambda = -0.1, n = 0.2, k = 1)$ remain mostly well within the 3σ region of the corresponding quantities as extracted from the observation. For other 3 sets of parameter values (λ, n, k) considered here, *viz.* (0.1, 1,1), (1,1,1), (10,1,1), the energy density curves are outside the corresponding 3σ range obtained from observation. A close look at the plots of pressure profile for exponential and logarithmic models in Fig. 5 reveals that the fluid pressure profile for exponential models also lies almost entirely within its the 3σ observed limits, for the full range of time (τ) accessible in SNe Ia observations, while for power law model, the corresponding curve is outside the 3σ observed limits for a small temporal regime during a relatively earlier part of late-time cosmic evolution. Therefore, non-minimally coupled matter-curvature scenarios with fluid pressure modelled as $p \sim e^{ak}$ mimics the outcome of the $\Lambda-$CDM model in terms of energy density and pressure profiles within their 3σ limits, for the model parameters taking values in the close proximity of the values $\lambda = -0.1, n = 0.2, k = 1$. We may mention here, that the $\Lambda-$CDM model which, though fits the data well, is plagued

with the coincidence and fine-tuning problems, whereas the models with non-minimally coupled matter-curvature scenarios are free from such problems.

In the light of the above results we also investigated the issue of energy transfer between curvature and fluid sectors owing to the considered non-minimal coupling between them. For the non-minimally coupled curvature-fluid models considered in this article, the energy-balance equation takes the form [50],

$$\nabla^{\mu}T_{\mu\nu} \;=\; \frac{\lambda F_2(R)}{1+\lambda f_2(R)}\Big(g_{\mu\nu}\mathcal{L}_m - T_{\mu\nu}\Big)\nabla^{\mu}R\,. \tag{24}$$

For an ideal fluid with energy density ρ and pressure p in FRW spacetime background and with $\mathcal{L}_m = p$ as considered in the work, the $\nu = 0$ component of Eq. (24) takes the form

$$\dot{\rho} + 3H(\rho + p) \;=\; -\frac{\lambda F_2(R)}{1+\lambda f_2(R)}\Big(p+\rho\Big)\dot{R} \equiv Q\,. \tag{25}$$

Note that, in absence of any non-minimal coupling ($\lambda = 0$), the above energy balance equation reduces to usual continuity equation $\dot{\rho} + 3H(\rho + p) = 0$ of FRW universe. The term Q on right hand side of Eq. (25) is a measure of rate of energy exchange between matter and curvature sectors. In the context of Eq. (25) we may mention that, thermodynamical implications of curvature-matter coupling scenarios at cosmological scales have been investigated in [50–52], where from the perspective of thermodynamics of open systems, the energy balance equation (25) has been interpreted to describe particle creation in FRW universe. Such an interpretation requires referring to the term $-Q/3H$ as the creation pressure p_c associated with the particle creation, so as to cast the energy balance equation in the form $\dot{\rho}+3H(\rho+p+p_c) = 0$, with creation pressure subject being to the constraint that $p_c \equiv -Q/3H < 0$, implying the requirement that Q always remains positive.

In the context of non-minimally coupled curvature-fluid models considered here with $f_2(R) = R^n$, we may write down the expression for the time profile of the Q-function from Eq. (25) corresponding to the parameter set (λ, n, k) as

$$Q(t;\lambda,n,k) \;=\; -\frac{\lambda n R^{n-1}}{1+\lambda R^n}\Big[p(t;\lambda,n,k) + \rho(t;\lambda,n,k)\Big]\dot{R} \tag{26}$$

where the energy density $\rho(t;\lambda,n,k)$ and fluid pressure $p(t;\lambda,n,k)$ profiles corresponding to both exponential and power law models are given by Eqs. (9) - (12). We use Eq. (26) to compute the function $Q(t;\lambda,n,k)$ for given choices of λ, n, k. Time dependences of cosmological parameters *viz.* a, H, R *etc.*, as extracted from observed data are instrumental in the determination of the temporal profile of Q. In Fig. 6 we have shown the time dependence of Q for both exponential (left panel) and power law (right panel) models by plotting $Q(\tau)/\rho_0$ vs τ for the same 4 benchmark values of parameters (λ, n, k) as taken earlier.

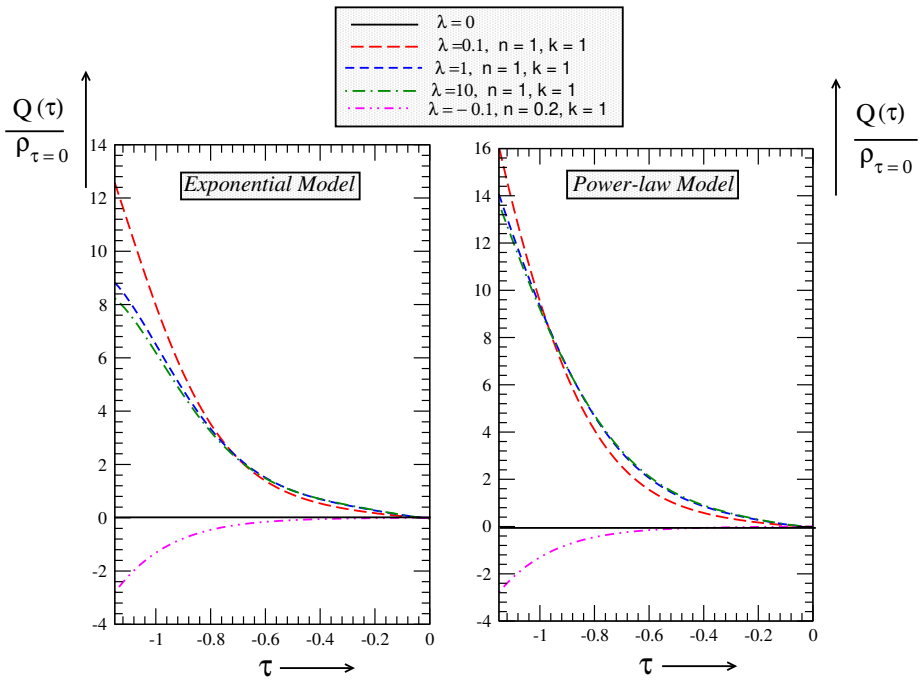


Figure 6: Temporal behaviour the function $Q(t;\lambda,n,k)$ (discussed in text) for different sets of benchmark values of parameters $Q(t;\lambda,n,k)$ for exponential (left panel) and power-law (right panel) models

We observe from Fig. 6 that, corresponding to the benchmark cases with $n = 1$ (*i.e.* $f_2(R) = R$) and $k = 1$ (which correspond to $p \sim e^a$ for exponential model and $p \sim a$ for power law model), $Q(\tau)$ remains always positive. So, certain domains of (λ, n, k) parameter space of non-minimally coupled matter-curvature models are allowed from the combined analysis of Pantheon data and OHD, for which the possibility of interpreting the energy balance equation in terms of particle creation [50] remains open. On the other hand, the estimation of $Q(\tau)$ for parameter values $(\lambda = -0.1, n = 0.2, k = 1)$, (which mimics energy density and pressure profile obtained from the data analysis with Λ-CDM model as explained earlier) gives negative values of Q for the entire time range probed in SNe Ia observations. We also observe from Fig. 6 that, the absolute value of the rate of energy transfer between curvature and matter sectors and hence the effect of the considered non-minimal coupling, monotonically decreases as time approaches towards the present epoch.

5 Conclusion

In this work we considered non-minimally coupled curvature-matter models of gravity and investigated its cosmological implications in the light of luminosity distance and redshift measurements of Supernova Ia events. The non-minimal curvature-matter coupling has been introduced by adding a term $\int [\lambda R^n \mathcal{L}_m] \sqrt{-g} d^4x$ to the usual action for Einstein's gravity involving the Einstein Hilbert action and minimally coupled matter action. The parameters λ and n fix the strength and nature of the non-minimal coupling. To explore consequences of such non-minimal couplings in relation to evolutionary aspects of the universe at large scales, we considered homogeneous and isotropic spacetime geometry of the expanding universe described by a flat FRW metric involving the time dependent scale factor $a(t)$. The matter content of the universe is modelled as a perfect fluid characterised by energy density $\rho(t)$ and pressure $p(t)$ and chosen

the form of matter Lagrangian as $\mathcal{L}_m = p$. Such a choice for Lagrangian density correctly reproduces the hydrodynamical equations for the perfect fluid and also may cause to vanish the extra force owing to departure from motion along the geodesic arising from a non-vanishing covariant derivative of energy-momentum tensor in coupled scenarios. For such considerations, the field equations corresponding to the modified action containing non-minimal term take forms exhibiting connection between the $a(t), \rho(t), p(t)$ through their time derivatives and various other functions like the Hubble function $H(t)$ and the Ricci scalar $R(t)$. The functions $H(t)$, $R(t)$ are however also directly related to the scale factor $a(t)$ and its derivatives. The evolution equations also involve the parameters λ and n related to the curvature-matter coupling and the minimal coupling scenario corresponds to $\lambda = 0$, for which the equations reduce to the Friedman equations. Unlike Friedman's equations, their corresponding analogues which govern the evolutionary dynamics in presence of non-minimal curvature-matter coupling, involves time derivates of fluid pressure p. We investigate the observational constraints on the non-minimal models choosing two different ansatzes for $p(t)$ referred to in the paper as the 'exponential model' and 'power law model', where the temporal profile of the fluid pressure has been parametrized in terms of a dimensionless parameter k as $p \sim e^{ka}$ and $p \sim a^k$ respectively. Consequently, in the context of this work, the interplay of the three parameters (λ, n, k) plays a pivotal role in testing the consistency of non-minimally coupled fluid-curvature scenarios with the observed data.

From a comprehensive analysis of Pantheon compilation of 1048 SNe Ia data points and 54 data points on measurement of Hubble parameter from OHD, we obtained time dependences of the relevant cosmological parameters $a(t), H(t), R(t)$ and their time derivatives over the late time phase of cosmic evolution. Taking into account all these information and using the evolution equations for non-minimally coupled scenarios, we numerically computed the energy density $\rho(t, \lambda, n, k)$ and pressure $p(t, \lambda, n, k)$ profiles for different values of (λ, n, k) thoroughly scanning a portion of the parameter space: $[-0.1 \leqslant \lambda \leqslant 10; -10 \leqslant n \leqslant 10; -20 \leqslant k \leqslant 10]$. We also obtained and presented in Fig. 4, the regions in the parameter space corresponding to parameter values giving $\rho(t, \lambda, n, k) > 0$ for all t which is a trivial but essential requirement for viability of cosmological models. We found there exist large domains in the (λ, n, k)-parameter space for which models with non-minimal curvature-matter mixing stand as viable cosmological models reproducing the observed features of late time cosmic evolution. We have also seen that there exist a small range of parameter values around $(\lambda = -0.1, n = 0.2, k = 1)$ for which the computed temporal profiles of ρ and p mimic the corresponding profiles obtained from the analysis of the data using $\Lambda-$CDM model in the context of usual minimal coupling scenario.

The energy-momentum tensor has a non-vanishing covariant derivative ($\nabla^\mu T_{\mu\nu} \neq 0$) in the realm of non-minimally coupled curvature-matter scenarios and this implies exchange of energy between curvature and matter sectors. We found that, the absolute value of the rate of energy transfer between the two sectors monotonically decreases as time approaches towards the present epoch. This dynamics of energy exchange may be expressed by an equation portraying the energy balance between the two sectors in FRW background as $\dot{\rho}+3H(\rho+p+p_c) = 0$, with the function $p_c(t)$ (multiplied by $3H$) providing a measure of the rate of energy transfer owing to the non-minimal coupling between curvature and matter. From the perspective of thermodynamics of open systems, as extensively discussed in [50–52], curvature-matter coupling allows production of a substantial amount of comoving entropy during late time evolutionary phase of the universe. This opens up the possibility to interpret the energy-balance equation describing particle creation in FRW universe, with p_c realised as the (creation) pressure related to the particle creation. Such an interpretation however requires p_c to be negative. Our investigation shows, there exist values of model parameters (λ, n, k), for which the requirement $p_c < 0$ (for all time) is met. Thus the 'particle creation' interpretation of energy balance equation in non-minimally coupled

curvature-matter scenarios remains an open possibility in the context of SNe Ia data.

Acknowledgement We express our gratitude to the referees for providing valuable suggestions. A.C. would like to thank Indian Institute of Technology, Kanpur for supporting this work by means of Institute Post-Doctoral Fellowship **(Ref.No.DF/PDF197/2020-IITK/970)**.

References

[1] A. G. Riess *et al.* [Supernova Search Team], Astron. J. **116**, 1009 (1998) doi:10.1086/300499 [astro-ph/9805201].

[2] S. Perlmutter *et al.* [Supernova Cosmology Project Collaboration], Astrophys. J. **517**, 565 (1999) doi:10.1086/307221 [astro-ph/9812133].

[3] Y. Sofue and V. Rubin, Ann. Rev. Astron. Astrophys. **39**, 137 (2001).

[4] M. Bartelmann and P. Schneider, Phys. Rept. **340**, 291 (2001).

[5] D. Clowe, A. Gonzalez and M. Markevitch Astrophys. J. **604**, 596 (2004).

[6] G. Hinshaw *et al.* [WMAP], Astrophys. J. Suppl. **180** (2009), 225-245 doi:10.1088/0067-0049/180/2/225 [arXiv:0803.0732 [astro-ph]].

[7] P. A. R. Ade *et al.* [Planck], Astron. Astrophys. **571** (2014), A16 doi:10.1051/0004-6361/201321591 [arXiv:1303.5076 [astro-ph.CO]].

[8] I. Zlatev, L. M. Wang and P. J. Steinhardt, Phys. Rev. Lett. **82** (1999), 896-899 doi:10.1103/PhysRevLett.82.896 [arXiv:astro-ph/9807002 [astro-ph]]

[9] J. Martin, Comptes Rendus Physique **13** (2012), 566-665 doi:10.1016/j.crhy.2012.04.008 [arXiv:1205.3365 [astro-ph.CO]].

[10] R. D. Peccei, J. Sola and C. Wetterich, Phys. Lett. B **195** (1987), 183-190 doi:10.1016/0370-2693(87)91191-9

[11] L. H. Ford, Phys. Rev. D **35** (1987), 2339 doi:10.1103/PhysRevD.35.2339

[12] P. J. E. Peebles and B. Ratra, Rev. Mod. Phys. **75** (2003), 559-606 doi:10.1103/RevModPhys.75.559 [arXiv:astro-ph/0207347 [astro-ph]].

[13] T. Nishioka and Y. Fujii, Phys. Rev. D **45** (1992), 2140-2143 doi:10.1103/PhysRevD.45.2140

[14] P. G. Ferreira and M. Joyce, Phys. Rev. Lett. **79** (1997), 4740-4743 doi:10.1103/PhysRevLett.79.4740 [arXiv:astro-ph/9707286 [astro-ph]].

[15] P. G. Ferreira and M. Joyce, Phys. Rev. D **58** (1998), 023503 doi:10.1103/PhysRevD.58.023503 [arXiv:astro-ph/9711102 [astro-ph]]

[16] R. R. Caldwell, R. Dave and P. J. Steinhardt, Phys. Rev. Lett. **80** (1998), 1582-1585 doi:10.1103/PhysRevLett.80.1582 [arXiv:astro-ph/9708069 [astro-ph]].

[17] S. M. Carroll, Phys. Rev. Lett. **81** (1998), 3067-3070 doi:10.1103/PhysRevLett.81.3067 [arXiv:astro-ph/9806099 [astro-ph]]

[18] E. J. Copeland, A. R. Liddle and D. Wands, Phys. Rev. D **57** (1998), 4686-4690 doi:10.1103/PhysRevD.57.4686 [arXiv:gr-qc/9711068 [gr-qc]].

[19] W. Fang, H. Tu, Y. Li, J. Huang and C. Shu, Phys. Rev. D **89** (2014) no.12, 123514 doi:10.1103/PhysRevD.89.123514 [arXiv:1406.0128 [gr-qc]].

[20] C. Armendariz-Picon, T. Damour and V. F. Mukhanov, Phys. Lett. B **458** (1999), 209-218 doi:10.1016/S0370-2693(99)00603-6 [arXiv:hep-th/9904075 [hep-th]]

[21] C. Armendariz-Picon, V. F. Mukhanov and P. J. Steinhardt, Phys. Rev. D **63** (2001), 103510 doi:10.1103/PhysRevD.63.103510 [arXiv:astro-ph/0006373 [astro-ph]]

[22] C. Armendariz-Picon, V. F. Mukhanov and P. J. Steinhardt, Phys. Rev. Lett. **85** (2000), 4438-4441 doi:10.1103/PhysRevLett.85.4438 [arXiv:astro-ph/0004134 [astro-ph]]

[23] C. Armendariz-Picon and E. A. Lim, JCAP **08** (2005), 007 doi:10.1088/1475-7516/2005/08/007 [arXiv:astro-ph/0505207 [astro-ph]]

[24] T. Chiba, T. Okabe and M. Yamaguchi, Phys. Rev. D **62** (2000), 023511 doi:10.1103/PhysRevD.62.023511 [arXiv:astro-ph/9912463 [astro-ph]]

[25] N. Arkani-Hamed, H. C. Cheng, M. A. Luty and S. Mukohyama, JHEP **05** (2004), 074 doi:10.1088/1126-6708/2004/05/074 [arXiv:hep-th/0312099 [hep-th]]

[26] R. R. Caldwell, Phys. Lett. B **545** (2002), 23-29 doi:10.1016/S0370-2693(02)02589-3 [arXiv:astro-ph/9908168 [astro-ph]]

[27] S. Capozziello, Int. J. Mod. Phys. **D11**, 483 (2002); S. Capozziello, V. F. Cardone, S. Carloni, and A. Troisi, Int. J. Mod. Phys. **D12**, 1969 (2003); ; S. Nojiri and S. D. Odintsov, Phys. Rev. D **68**, 123512 (2003); S. Nojiri and S. D. Odintsov, Phys. Rept. **505**, 59 (2011); S. Nojiri, S. D. Odintsov and V. K. Oikonomou, Phys. Rept. **692**, 1 (2017)

[28] D. M. Scolnic *et al.* [Pan-STARRS1], Astrophys. J. **859** (2018) no.2, 101 doi:10.3847/1538-4357/aab9bb [arXiv:1710.00845 [astro-ph.CO]]

[29] Blake C *et al.* 2012 Mon. Not. R. Astron. Soc. 425 405–14

[30] Chuang C-H and Wang Y 2013 Mon. Not. R. Astron. Soc. 435 255–62

[31] Font-Ribera A *et al.* 2014 J. Cosmol. Astropart. Phys. JCAP05(2014)027

[32] Delubac T *et al.* 2015 Astron. Astrophys. 574 A59

[33] Bautista J E *et al.* 2017 Astron. Astrophys. 603 A12

[34] O. Bertolami, F. S. N. Lobo and J. Paramos, Phys. Rev. D **78**, 064036 (2008) doi:10.1103/PhysRevD.78.064036 [arXiv:0806.4434 [gr-qc]]

[35] B. F. Schutz, Phys. Rev. D 2, 2762 (1970)

[36] J. D. Brown, Class. Quantum Gravity 10, 1579 (1993)

[37] O. Bertolami, C. G. Boehmer, T. Harko and F. S. N. Lobo, Phys. Rev. D 75, 104016 (2007)

[38] O. Bertolami and J. Paramos, Phys. Rev. D **77** (2008), 084018 doi:10.1103/PhysRevD.77.084018 [arXiv:0709.3988 [astro-ph]]

[39] T. P. Sotiriou, Phys. Lett. B **664** (2008), 225-228 doi:10.1016/j.physletb.2008.05.050 [arXiv:0805.1160 [gr-qc]]

[40] O. Bertolami and J. Paramos, Class. Quant. Grav. **25** (2008), 245017 doi:10.1088/0264-9381/25/24/245017 [arXiv:0805.1241 [gr-qc]]

[41] R. P. Azevedo (2022), Cosmological Implications of Nonminimally-Coupled $f(R)$ Gravity and the Lagrangian of Cosmic Fluids. [arXiv. /abs/2207.08578 [gr-qc]]

[42] P. P. Avelino & R. P. L. Azevedo, Phys. Rev. D **97**, 64018 (2018). doi: 10.1103/PhysRevD.97.064018. 1002.4928

[43] R. P. L. Azevedo & P. P. Avelino, Phys. Rev. D **99**, 064027 (2019). doi: /10.1103/PhysRevD.99.064027

[44] R. P. L. Azevedo and P. P. Avelino, EPL **132** (2020) no.3, 30005 doi:10.1209/0295-5075/132/30005 [arXiv:1908.02629 [gr-qc]].

[45] S. Thakur & A. A. Sen, Phys. Rev. D **88**, 044043 (2013). doi: 10.1103/PhysRevD.88.044043

[46] R. K. Tiwari, B. K. Shukla, D. Sofuoğlu and D. Kösem, Symmetry **15** (2023) no.4, 788 doi:10.3390/sym15040788

[47] V. Faraoni, Phys. Rev. D **76** (2007), 127501 doi:10.1103/PhysRevD.76.127501 [arXiv:0710.1291 [gr-qc]]

[48] T. P. Sotiriou and V. Faraoni, Class. Quant. Grav. **25** (2008), 205002 doi:10.1088/0264-9381/25/20/205002 [arXiv:0805.1249 [gr-qc]]

[49] S. W. Hawking and G.F.R. Ellis, The Large Scale Struc- ture of Spacetime, (Cambridge University Press, Cam- bridge 1973)

[50] T. Harko, F. S. N. Lobo, J. P. Mimoso and D. Pavón, Eur. Phys. J. C **75** (2015), 386 doi:10.1140/epjc/s10052-015-3620-5 [arXiv:1508.02511 [gr-qc]]

[51] T. Harko, Phys. Rev. D **90** (2014) no.4, 044067 doi:10.1103/PhysRevD.90.044067 [arXiv:1408.3465 [gr-qc]]

[52] P. H. R. S. Moraes, R. A. C. Correa and G. Ribeiro, Eur. Phys. J. C **78** (2018) no.3, 192 doi:10.1140/epjc/s10052-018-5655-x [arXiv:1606.07045 [gr-qc]]

[53] J. A. Frieman, B. Bassett, A. Becker, C. Choi, D. Cinabro, D. F. DeJongh, D. L. Depoy, M. Doi, P. M. Garnavich and C. J. Hogan, *et al.* Astron. J. **135** (2008), 338-347 doi:10.1088/0004-6256/135/1/338 [arXiv:0708.2749 [astro-ph]]

[54] P. Astier *et al.* [SNLS], Astron. Astrophys. **447** (2006), 31-48 doi:10.1051/0004-6361:20054185 [arXiv:astro-ph/0510447 [astro-ph]]

[55] M. Hicken *et al.*, ApJ **700** (2009), 331 doi: 10.1088/0004-637X/700/1/331 [arXiv:0901.4787]

[56] A. G. Riess, L. G. Strolger, S. Casertano, H. C. Ferguson, B. Mobasher, B. Gold, P. J. Challis, A. V. Filippenko, S. Jha and W. Li, *et al.* Astrophys. J. **659** (2007), 98-121 doi:10.1086/510378 [arXiv:astro-ph/0611572 [astro-ph]]

[57] G.A. Baker Jr. and P. Graves-Morris, Pade Approximants, Cambridge University Press (1996).

[58] A. Bandyopadhyay, D. Gangopadhyay, A. Moulik, Eur. Phys. J. C 72, 1943 (2012)

[59] Wei J-J 2018 Model-independent curvature determination from gravitational-wave standard sirens and cosmic chronometers Astrophys. J. 868 29

[60] Foreman-Mackey D, Hogg D W, Lang D and Goodman J 2013 Publ. Astron. Soc. Pac. 125 306–12

[61] Lewis A 2019 GetDist: a Python package for analysing Monte Carlo samples (arXiv:1910.13970 [astro-ph.IM])